

DESIGN MANUAL DEVELOPMENT FOR THE 36-INCH DOUBLE-WEB BEAM

Timothy J. Schniepp, Michael D Hayes, John J. Lesko & Thomas E. Cousins

Department of Engineering Science and Mechanics

Virginia Tech

Blacksburg, VA 24061

(540) 231-3139

Fax: (540) 231-9187

tschniep@vt.edu

Abstract

Fiber-reinforced polymeric (FRP) composites are being considered for structural members in bridge construction as lighter, more durable alternatives to steel and concrete. Extensive testing and analysis of a pultruded, hybrid double web beam (DWB) developed for use in bridge construction has been conducted at Virginia Tech. A primary purpose of this testing is the development of a structural design guide for the DWB, which includes stiffness and strength data. The design manual also includes design allowables determined through a statistical analysis of test data.

Static testing of the beams, including failure tests, has been conducted in order to determine such beam properties as bending modulus, shear stiffness, failure mode, and ultimate capacity. Measuring and calculating the shear stiffness has proven to be an area of particular interest and difficulty. Shear stiffness is calculated using Timoshenko beam theory which combines the shear stiffness and shear area together along with a correction factor, k . There are several methods for determining shear stiffness, kGA , in the laboratory, including a direct method and a multi-span slope method. Herein lays the difficulty as it has been found that varying methods produces significantly different results. The objective of current research is to determine reasons for the differences in results, to identify which method is most accurate in determining kGA and also to examine higher-order theories that may further aid the understanding of this material property.

This paper will outline the development of the design guide, the philosophy for the selection of allowables and review and discuss the challenges of interpreting laboratory data to develop a complete understanding of shear effects in large FRP structural members.

Introduction

FRP Composites in Infrastructure

Fiber-reinforced polymeric (FRP) composites are being considered for structural members in bridge construction as lighter, more durable alternatives to steel and concrete. The interest in these materials can be attributed to the ability of FRP to better meet the performance and durability needs of current construction. Existing structural shapes include wide-flange beams, box beams, sandwich beams, and multi-cellular panels. The constituent materials of these structural components tend to be E-glass fibers and low cost resin systems (polyester, vinyl ester, etc.). Occasionally, carbon fiber is utilized in flanges or face sheets in order to increase bending stiffness. Construction typically occurs using off-the-shelf pultruded sections or structural members may be manufactured using vacuum-assisted resin transfer molding. The benefits of FRP for use in infrastructure compared to conventional materials are high strength to weight ratios, high corrosion resistance, lightweight, electromagnetic transparency, and excellent fatigue performance [1].

Design of FRP structures is typically deflection or stiffness limited. Since the lower modulus of FRP materials (relative to steel) results in greater deflections, problems may develop for overlay and connection durability. As a result of meeting stiffness criterion, FRP structures will typically provide a high factor of safety on strength initially. For this reason, long-term durability of FRP in primary load-bearing applications has not been adequately addressed. However, although FRP does not rust, a change of state or degradation can occur due to hygrothermal aging, UV exposure, mechanical fatigue, etc.

A number of studies have focused on the static performance and failure modes of fiberglass structures, but few have considered the fatigue performance or environmental durability of such systems. Most durability work has been limited to coupon-level studies and the development of life predictions for the structure based on the kinetics of damage mechanisms in coupon specimens has not been attempted. Furthermore, due to the presence of geometric and material discontinuities, failure often occurs by way of face/flange compression, web buckling, or delamination at an interface rather than fiber fracture at the ply level. Therefore, macro-level coupon studies may fail to predict the ultimate failure stresses in a structural component. Currently, research is being conducted at Virginia Tech to fill this niche by developing strength and life predictions for FRP structures that may fail due to a number of possible failure modes including delamination.

Hybrid Double-Web Beam

Strongwell Corporation of Bristol, Virginia has developed a 36-inch deep pultruded double web beam (DWB) for use in bridge construction (Figure 1). The beam is a hybrid laminated composite, composed of both E-glass and carbon fibers in a vinyl ester resin. As a demonstration of the technology, a 40-ft long single-span bridge in Marion, Virginia was rehabilitated in Summer 2001 using eight double web beams. Prior to the rehabilitation, the beams to be implemented in the new structure were tested quasi-statically to obtain stiffness data. Failure testing of additional beams has also been conducted and is nearing completion.

During the development of the 36-inch DWB, an 8-inch deep subscale prototype was studied and implemented in the Tom’s Creek Bridge rehabilitation in 1997 [1]. The results of extensive testing of this section including stiffness and strength data have been published in a structural design guide, published in 2000 [2]. As tested in three- and four-point bending, the 8-inch DWB

consistently fails by Delamination within the compressive flange at the interface between carbon and glass fibers. The critical stress in this case is thought to be the normal, out-of-plane stress at the free edges. Furthermore, the delamination appears to initiate at the load points, suggesting that load concentrations have a significant effect on the critical stress. Therefore, an analytical model that can accurately predict ply-level stresses at the free edge and account for concentrated loading is required.

36-Inch DWB Structural Design Guide

As it was previously stated, failure testing of the 36-inch DWB is nearing completion. The primary purpose of this testing is the development of a structural design guide for the DWB, which will

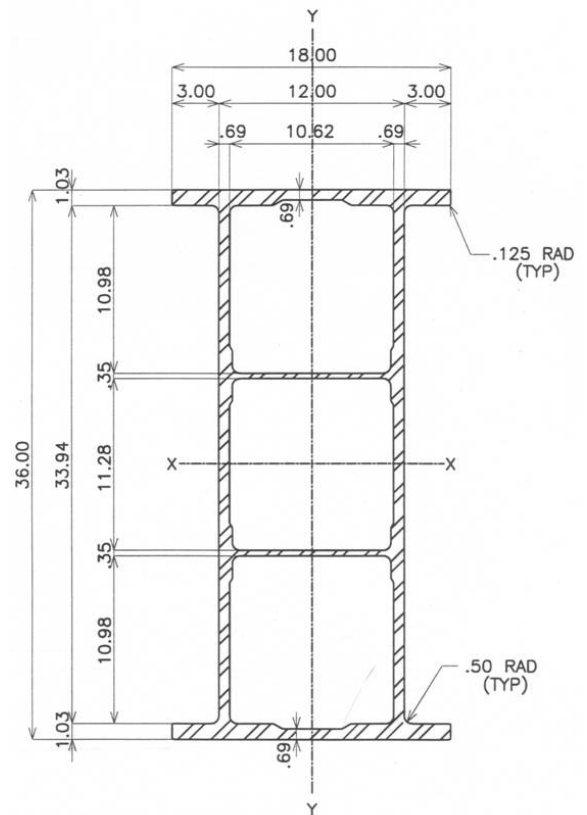


Figure 1. Strongwell's 36" DWB

contain strength and stiffness data obtained during testing. The design guide is presented as a material specification where the material system and the manufacturing process are well defined and controlled. Knowing the tolerances of this system and process, guidelines are defined for the use of the structural member. As a basis for defining operating limits, a modified Load Resistance Factor Design (LRFD) approach is used [3]. For this approach the probability distribution of loads/stress (Loads, Q) is compared to the probability of failure strength of the material (Resistance, R), typically represented as illustrated in Figure 2. The region of overlap is *related* to the risk associated with the situation designed. Specifically in the design guide, the resistance portion of the design problem is presented by employment of Weibull statistics on test data. Weibull statistics help capture the variability of materials by describing the probability of failure. A reliability based selection approach is used, from the recorded variability of girder test data, to define A- and B-basis allowable levels of resistance. These values define for users of the design guide the level of risk allowed in operating the structure based on a determined design load. The difference between the selected design loads and the resistance defined as a probability of failure load/stress defines the level of risk (or inversely the margin of safety) for the design, as illustrated in Figure 2.

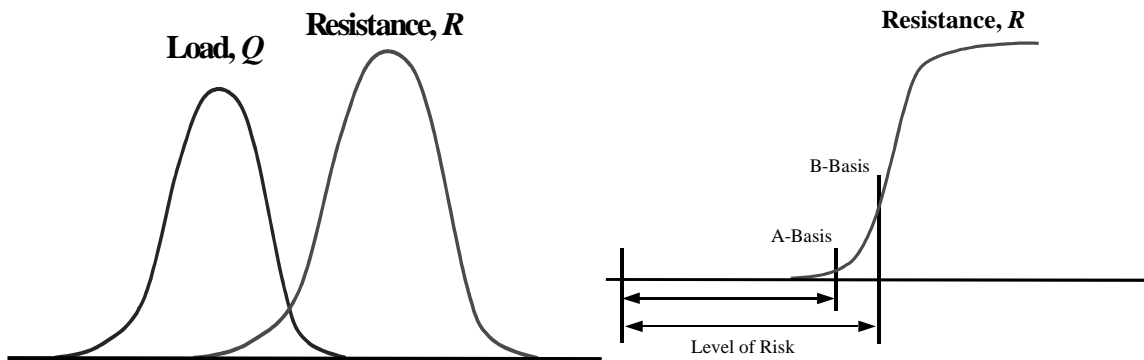


Figure 2. LRFD conceptual representation for design; A- and B-Basis Allowables

The purpose of the design guide is to assist potential users of the DWB in specifying the component in various structural applications. The content includes the specification of bending stiffness, shear stiffness, moment capacity, lateral-torsional stability, bearing capacity, and bolted connection specifications. Currently, research and testing is being done on a number of these member properties and specifications. An overview of the testing and results follows below.

Experimental Setup

As a precursor to the strength testing of the 36-inch DWB, a number of tests were performed on the 8-inch DWB. Preliminary results from strength testing the 8-inch DWB indicated that the moment to failure varied with shear span or clear span. In order to further examine the contribution of span (and therefore shear) to the failure of the 8-inch DWB, a number of three-point, short-span failure tests were performed. Spans of 16, 32 and 60 inches (corresponding to 2, 3 and 7.5 times the depth of the beam) were chosen. Data at longer spans of 8, 14 and 17.5 feet (length-to-depth ratios of 12, 21 and 26, respectively) had been previously collected. For the short beam tests, three beams of each length were loaded to failure in a three-point bend test geometry (Figure 3). Six-inch square, a 1-inch thick elastomeric bearing pad was used at the load point (and similar, thinner pads at the end supports) to distribute the load evenly; a 1-inch thick steel plate under the actuator was also utilized. The ends were restrained to prevent any lateral translation. Deflection was measured at mid-span using a wire

potentiometer. Shear strain in the web near the loading point was measured in one test at each span with strain gages placed at a $\pm 45^\circ$ orientation along the neutral axis of the beam underneath the load patch and outside the patch at a distance of at least one pad's width in order to examine the effect of a concentrated load on the local stress field, i.e. the degree to which cross-sectional warping affects the flange stresses.



Figure 3. Short span three-point bending test setup

The primary purpose of this short span testing was to establish the dependency on span of the shear capacity of the 8-inch DWB and use that information to predict the capacity of the 36-inch DWB. The shear capacity of the 8-inch beam versus the length-to-depth ratio as well as the initial prediction for the 36-inch beam can be seen below in Figure 4.

This prediction, which was made using a ratio of the capacity for the 8-inch DWB to the one known experimentally determined capacity for the the 36-inch DWB (i.e. the data point of the previously failed 39-ft girder) and then extending that relationship for the known values of the 8-inch DWB, was used to determine which spans of the 36-inch girder to select for failure tests. After taking into consideration the capacity of the test set-up available, spans of roughly 20, 40, and 60 feet were selected as it was thought that this would provide adequate data to compare to the predicted relationship between shear capacity and span. Due to various factors on the laboratory floor (available space, bolt hole locations, etc.), the spans at which the girders were actually initially tested were 18, 39, and 58 feet (length-to-depth ratios of 6, 13, and $19 \frac{1}{3}$, respectively). Seventeen girders (five to six beams of each span from three different manufacturing batches) were initially scheduled to be tested and failed. After testing girders at the aforementioned spans, an additional beam at a span of 30 feet (an aspect ratio of 10) was tested and further testing at this span is planned.

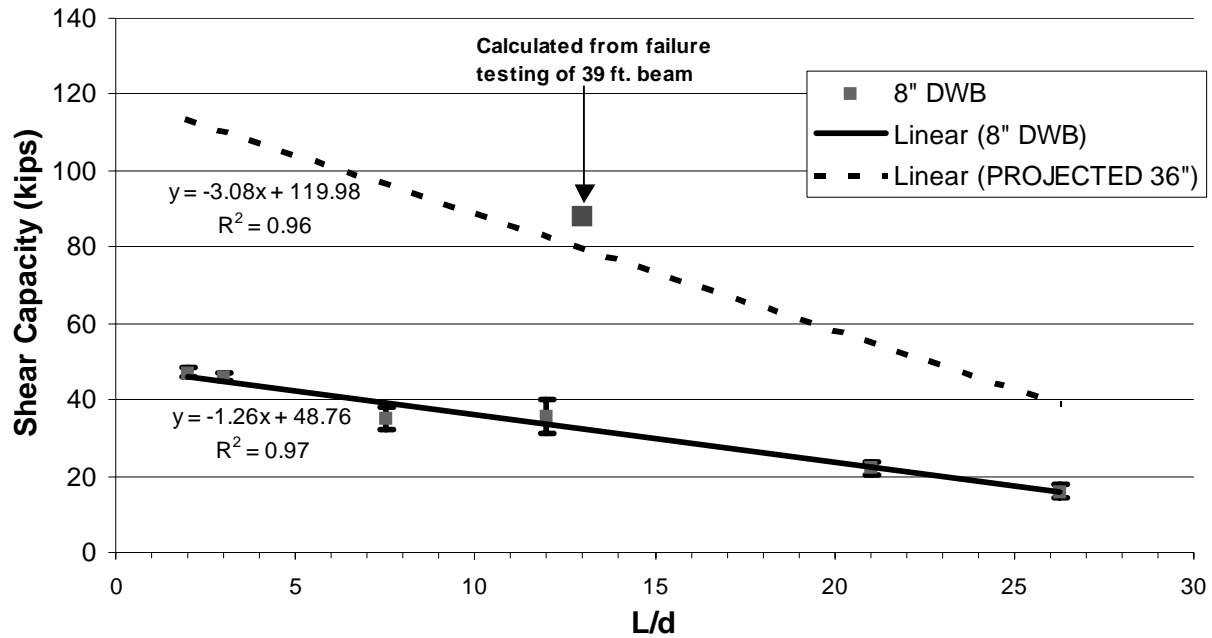


Figure 4. Shear capacity vs. L/d for 8-inch DWB and *initial* prediction for the 36-inch DWB

For the failure testing of the 36-inch DWB a four-point bending setup was utilized. The test setup involves two actuators located at roughly the third points with two 9- by 14-inch long elastomeric bearing pads (used to mimic bridge applications) at both the supports and the loading points (Figure 5). Thus, the load is applied through a fairly wide patch area. Displacement was measured at the midspan of each beam and at the quarter points for the 60-foot span. The end deflections (which occur due to the use of the elastomeric bearing pads) at the supports were also measured and subsequently subtracted from midspan deflections to find the net deflection of the girder. A variety of different strain gauging plans were implemented on the different beams of each span. On every beam, gauges were placed on the top and bottom flange at midspan to measure bending strain and axial gauges were placed on the web along the neutral axis to monitor for any warping in the beam. As with the 8-inch DWB, shear strain in the web was also measured under the load points and over the supports for beams at each span in order to examine the effect of a concentrated load on the local stress field.



Figure 5. Four-point bending test setup of 36-inch DWB

Results

As in previous testing, all girders demonstrated a linear-elastic response. As it was seen in the plot of shear capacity versus aspect ratio, a linear relationship between shear capacity and span exists for the 8-inch DWB (Figure 4). Initial testing of the larger girder at the 40- and 60-ft spans supported the hypothesis that the 36-inch DWB would behave in a similar fashion. Furthermore, the failure mechanism did not change at these two spans, just as it did not with the 8-inch girder. The 36-inch DWB appears to fail in a similar manner to the 8-inch DWB, which consistently fails by delamination in the top flange at a carbon-glass interface, beginning in the vicinity of the loading patches and progressing outward in both directions along the primary beam axis. Although for the 36-inch DWB, delamination may also initiate at the internal ply drop-off underneath the flange (refer to Figure 1). This drop-off is the result of glass fabrics in the outer half of each web that fold over in the pultrusion die to form the inner half of each flange. Further tests using crack detection gages to capture the path of crack growth along the length of the beam are planned, and non-destructive evaluation techniques are being investigated in order to identify the path of the debond across the width of the flange.

Testing for the 36-inch DWB began at the 60-foot span, progressed to the 40-foot girders, and then finally to the 20-foot beams. As it was mentioned, testing of the two longer spans supported the original hypothesis that failure was controlled by shear capacity, that this shear capacity varied linearly with span, and that the failure mechanism remained constant at different spans. Testing of the 20-foot DWBs revealed that this was not exactly the case. Three 20-foot, 36-inch DWBs were tested and all three failed by a different failure mechanism than the previously tested girders. It seems that shear capacity is not the only controlling factor as bearing failures were reached in all three of the 20-foot beams. The bearing failures occur at the end supports as a result of the elastomeric bearing pads

creating additional stresses on the flanges, causing cracking at the web-flange junction. In the worst case, the crack propagated up the web of the beam, causing it to buckle as seen below (Figure 7).



Figure 6. Delamination of the compressive flange of a 36-inch DWB near a loading patch.

Three different orientations of the elastomeric bearing pads were tried (one on each of the three girders tested), as it was thought that the original alignment created an upward stress on the flange edge that was causing the cracking at the web-flange junction. The original pad orientation (used for the 40- and 60-foot spans) was such that the pads stuck out 5 inches on each side of the beam, relative to the 18 inch width of the beam (the pads were 9 inches along the length of the beam and 28 inches across the width). The second orientation turned the pads so that they went from flange edge to flange edge (14 inches along the beams length, 18 inches across the width). It was thought that this may alleviate some of the stress on the flange edges, testing revealed that it did not. On the third and final 20-foot girder tested, only one bearing pad was used, centered under the beam so that the pad edges lined up exactly with the webs of the beam (14 inches across the width) and was 9 inches along the length of the beam. The bearing failure seen in Figure 7 occurred under this boundary condition.

After it was discovered that a bending-type failure could not be obtained at the short 20-foot span, an additional failure test of a 30-foot span was conducted. The bearing pads were oriented in the same manner as the second 20-foot test (18 inches wide, 14 inches along the length of the beam) and the beam did indeed fail by delamination in the top flange, the same mode as those of the two longest spans. Plans to obtain and test more 36-inch DWBs at this span are currently underway. The resulting plot of shear capacity versus aspect ratio may be seen below (Figure 8). It must be noted that beams with an aspect ratio of 6 did not fail in shear capacity and are therefore represented on the plot as individual data points. It also would not be representative to plot the average of those three tests, as the test geometries were slightly different due to the different bearing pad orientations. The solid line on the plot of course represents a linear trend line of the average shear capacities at the 30-, 40-, and 60-foot spans. The

dashed line represents a possible limit controlled by bearing stresses. Research is currently underway to better establish where this limit actually occurs.

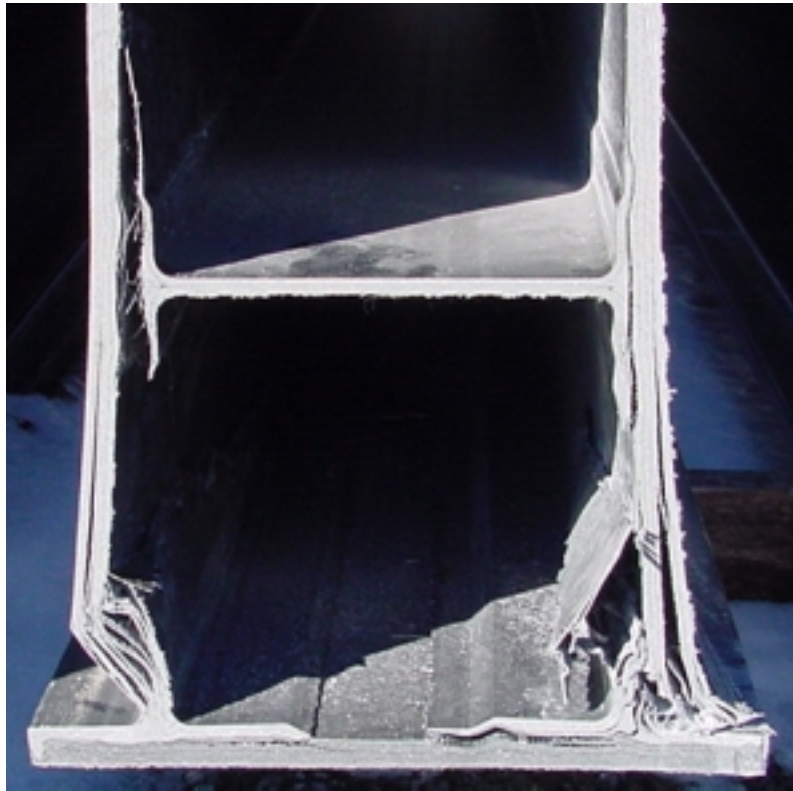


Figure 7. Bearing Failure of 36-inch DWB, 20-ft span

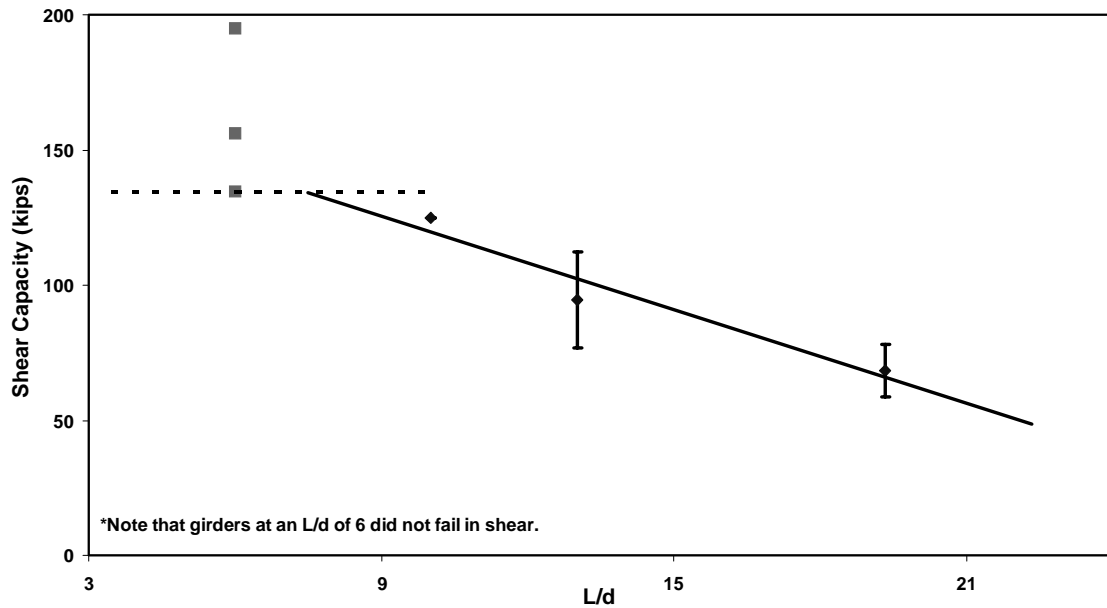


Figure 8. Average Shear Capacity versus L/d, 36-inch DWB, Error bars represent one standard deviation; Data points at L/d of 6 were bearing failures

In addition to examining the affect of span (and thus shear) on the failure of the 36-inch DWB, the purpose of the aforementioned failure testing was to obtain girder properties, such as strength and stiffness data, for the structural design guide. The testing provided various beam attributes, such as bending modulus, E, shear stiffness, kGA, ultimate capacity, failure moment, etc. and the *initial* results of analyzed data may be seen below (Figure 9).

In the summary table below, the column headed “Batch” refers to which of the three pultrusion runs that particular girder belongs (Batch 1—Summer 2000, Batch 2—May 2001, Batch 3—July 2001). The ultimate capacity was the total load of the two actuators that the beam supported at failure. The modulus referred to is the bending modulus, E, and kGA is the shear stiffness. Shear stiffness, kGA, was calculated using Timoshenko beam theory. As it can be seen, there is a relatively large amount of variation in shear stiffness, kGA. A great deal of current research is being dedicated to analyzing this variation. It has been found that kGA is extremely sensitive to small variations in measurements recorded during testing. For instance, kGA is calculated from and therefore directly dependent upon the measured deflection. Small variations in deflection result in drastically different kGA calculations. Changes as small as 3 to 4% in deflection can result in changes of kGA in excess of 50%. Since the ability to accurately measure deflection in the laboratory is limited by the sensitivity of equipment, some variation will obviously occur. This variation has led to problems in accurately calculating shear stiffness. As it was stated, these problems are being addressed in current research.

Beam	Batch	Span (ft.)	L/d	Shear Capacity (kips)	Ultimate Capacity (kips)	$M_{failure}$ (kip-ft)	Max ϵ_b ($\mu\epsilon$)	Modulus (msi)	kGA (psi*in ²)
1	3	18	6	156	312	994.5	2090	6.7	21
2	2	18	6	195	390	1283.8	2510	7.0	20
3	3	18	6	134.5	269	857.4	1850	6.5	20
1	1	30	10	121.5	243	1215.0	2540	6.8	20
0	1	39	13	88	176	1400.0	3150	6.2	25
1	3	39	13	113.5	227	1518.1	3440	6.3	45
2	3	39	13	72	144	963.0	2200	6.2	48
3	3	39	13	83	166	1110.1	lost data	6.0	55
4	3	39	13	106.5	213	1424.4	3150	6.5	40
5	1	39	13	117	234	1564.9	3570	6.6	41
6	1	39	13	81.5	163	1090.1	2570	6.3	46
1	2	58	19.33	82.5	165	1598.4	3660	6.4	53
2	2	58	19.33	73.5	147	1424.1	3170	6.7	30
3	2	58	19.33	59	118	1143.1	2620	6.4	38
4	3	58	19.33	60.5	121	1172.2	2620	6.3	43
5	3	58	19.33	66.5	133	1288.4	2930	6.4	45

Figure 9. Summary Table of data collected during 36-inch DWB testing; Note that 18-foot beams did not fail due to shear; Also note that values represent only an *initial* analysis of test data (further analysis is currently being conducted); Beam “zero” (39-foot section) was previously tested with slightly different test geometry; “Lost data” refers to data that was lost due to acquisition system failure

Future Research and Testing

The objective of current research is to explore and better understand the shear stiffness, kGA, of the 36-inch DWB. It is believed that a thorough understanding of this property has not yet been

attained. Current and future research in this area involves examining the methods used to obtain and calculate kGA (the direct and slope methods in particular), determining what method, if any, is most accurate, comparing results and resolving differences between methods (preliminary tests revealed large differences between methods), as well as examining higher order beam theories in order to better understand this material property. Small scale testing on box- and wide-flange beams is underway to determine the affects of varying such things as span, stiffness, geometry, etc. and using that information to better analyze the data for the 36-inch DWB as well as establishing with what accuracy kGA can be predicted analytically as those attributes are varied.

In addition to this research, further testing of the 36-inch DWB is also scheduled for Spring 2002. Both stability and fatigue testing of the girder are planned, the results of which will be included in the structural design guide for the girder. Also, due to the results of the failure testing of the 20-foot beams, more bearing failure tests are underway and additional failure testing at the 30-foot span will occur to better establish the dependency of shear capacity on span.

Summary

Experimental results from strength testing of the hybrid, 36-inch deep, composite double-web beam have been presented. The results indicate a strong dependence of ultimate strength upon shear capacity, with the exception being short spans, which appear to be controlled by bearing stresses. The failure mechanism for longer spans (L/d of 10+) of the 36-inch DWB appears to be delamination at the outer free edges of the compressive flange or the inner ply drop-offs on the compressive flange. Difficulty in consistently measuring shear stiffness, kGA, has occurred and is being addressed. Stability, fatigue, bearing, and additional failure testing of the 36-inch DWB is underway or planned. Results of this work will be forthcoming.

References

1. Hayes, M.D., Lesko, J.J., Weyers, R.E., Cousins, T.E., Haramis, J., Gomez, J. and Masarelli, P. 2000. "Laboratory and Field Characterization of the Tom's Creek Bridge Superstructure," *Journal for Composites in Construction*, 4(3): 120-128.
2. Strongwell. 2000. "EXTREN DWB™ Design Guide"
3. AASHTO (1998), LRFD Bridge Design Specification, 2nd edition, American Association of State Highway and Transportation Officials, Washington, D.C.
4. Hayes, M.D., T. Schniepp, and J.J. Lesko. Shear Effects in the Strength of FRP Structural Beams. in American Society of Composites Sixteenth Technical Conference. 2001. Blacksburg, Virginia: Technomic Publishing Co.
5. Hayes, M.D., Schniepp, T., Lesko, J.J., "Localized Effects in the Failure of FRP Structural Beams Tested in Transverse Loading," *Composite Materials: Testing and Design Fourteenth Volume, ASTM STP 1436*, C.E. Bakis, Ed., ASTM International, West Conshohocken, PA, 2003.
6. Nagaraj, V., "Static Behavior of Pultruded GFRP Beams", *Journal of Composites for Construction*, August 1997: 120-129.
7. Cowper, G.R., "The shear Coefficient in Timoshenko's Beam Theory", *Journal of Applied Mechanics*, June 1966: 335-340.
8. Weibull, Waloddi (1951), "A Statistical Distribution Function of Wide Applicability", *Journal of Applied Mechanics*, 293-297.
9. Weibull, Waloddi (1949), "A Statistical Representation of Fatigue Failures in Solids, Transitions of the Royal Institute of Technology", No. 27, Stockholm.